

NUMERICAL SIMULATION AND VALIDATION OF TURBULENT GAS-PARTICLE FLOW IN A BACKWARD-FACING STEP

K. MOHANARANGAM¹, J.Y. TU¹ and L. CHEN²

¹School of Aerospace, Mechanical and Manufacturing Engineering
 RMIT University, Vic. 3083, Australia

²Maritime Platforms division,
 DSTO, Maribyrnong, Vic. 3032, Australia

ABSTRACT

A numerical investigation into the particle-turbulence interaction behaviour of dilute gas-particle flows over a backward-facing step geometry is reported. An Eulerian two-fluid model with additional turbulence transport equations for particles is employed. RNG based k-ε model is used as the turbulent closure wherein additional transport equations are solved to better represent the combined gas-particle interactions. Three different particle classes are considered and their streamwise velocities and fluctuations are compared against the experimental data of Fessler & Eaton (1995).

INTRODUCTION

Dilute two-phase flows are found to be critical part in many industrial and mining processes, such as pneumatic transporters, pulverized coal combustion equipments, spray drying, cooling and also sand blasting. Numerical simulations of these classes of particle-laden flows are complicated by the fact that in addition to the modeling of single-phase turbulence, special considerations should also be made to incorporate particle interaction with the primary turbulent flow field.

In this paper, we present the results of the mean streamwise velocities; fluctuating velocities for both the carrier gas and particle phases, in addition particle number density (PND) results for different classes of particles considered are compared against the well established experimental data of Fessler and Eaton (1995). The re-attachment length for three particles along with two additional particles whose Stokes number is far less than other three has also been reported.

GOVERNING EQUATIONS

The Eulerian two-fluid model developed by Tu and Fletcher (1995) and Tu (1997) used in this study considers the gas and particle phases as two interpenetrating continua. Hereby, a two way coupling is achieved between the dispersed and the carrier phases.

The underlying assumptions employed in the current study are:

- 1) The particulate phase is dilute and consists of mono disperse spherical particles.
- 2) For such a dilute flow, the gas volume fraction is approximated by unity.
- 3) The viscous stress and the pressure of the particulate phase are negligible.
- 4) The flow field is isothermal.

Gas phase:

The governing equations in Cartesian form for steady, mean turbulent gas flow are obtained by Favre averaging the instantaneous continuity and momentum equations

$$\frac{\partial}{\partial x_i}(\rho_g u_g^i) = 0 \quad (1)$$

$$\frac{\partial}{\partial x_j}(\rho_g u_g^j u_g^i) = -\frac{\partial p_g}{\partial x_i} + \frac{\partial}{\partial x_j}(\rho_g (v_{gl} + v_{gt})) \frac{\partial}{\partial x_j} u_g^i - F_{Di} \quad (2)$$

Eq. (1) and (2) respectively are the continuity and momentum equation of the carrier gas phase, where ρ_g, u_g, u'_g and p_g are the bulk density, mean velocity, fluctuating velocity and mean pressure of the gas phase, respectively. v_{gl} is the laminar viscosity of the gas phase. F_{Di} is the Favre-averaged aerodynamic drag force due to the slip velocity between the two phases and is given by

$$F_{Di} = \rho_p \frac{f (u_g^i - u_p^i)}{t_p} \quad (3)$$

where the correction factor f is selected according to Schuh et al.(1989)

$$f = \begin{cases} 1 + 0.15 \text{Re}_p^{0.687} & 0 < \text{Re}_p \leq 200 \\ 0.914 \text{Re}_p^{0.282} + 0.0135 \text{Re}_p & 200 < \text{Re}_p \leq 2500 \\ 0.0167 \text{Re}_p & 2500 < \text{Re}_p \end{cases} \quad (4)$$

with the particle response or relaxation time given by $t_p = \rho_p d_p^2 / (18 \rho_g \nu_{gl})$, wherein d_p is the diameter of the particle.

The carrier gas phase uses an eddy-viscosity model, in which ν_{gt} is the turbulent or 'eddy' viscosity of the gas phase, which is computed by $\nu_{gt} = C_\mu (k_g^2 / \epsilon_g)$. This is achieved by separately solving transport equations for kinetic energy (k_g) and dissipation rate (ϵ_g) as per the RNG theory (Yakhot and Orszag 1986).

Particulate Phase:

After Favre averaging, the steady form of the governing equations for the particulate phase is

$$\frac{\partial}{\partial x_i}(\rho_p u_p^i) = 0 \quad (5)$$

$$\frac{\partial}{\partial x_j}(\rho_p u_p^j u_p^i) = -\frac{\partial}{\partial x_j}(\rho_p \overline{u_p^j u_p^i}) + F_{Gi} + F_{Di} + F_{WMi} \quad (6)$$

where ρ_p, u_p and u'_p are the bulk density, mean and fluctuating velocity of the particulate phase, respectively. In equation (12), there are three additional terms representing the gravity force, aerodynamic drag force, and the wall-momentum transfer force due to particle-wall collisions, respectively. The gravity force is $F_{Gi} = \rho_p g$, where g is the gravitational acceleration.

NUMERICAL PROCEDURE

The simulated results are compared against the experimental data of Fessler & Eaton (1999) for a gas-particle flow in a backward-facing step. Three classes of particles are considered in the study, their material properties and also their characteristics are tabulated in Table 1. The governing transport equations are discretized using a finite-volume approach. The equations are solved on a nonstaggered grid system. Third-order QUICK scheme is used to approximate the convective terms, while second-order accurate central difference scheme is adopted for the diffusion terms. The velocity correction is realized to satisfy continuity through SIMPLE algorithm, which couples velocity and pressure. At the inlet boundary the particulate phase velocity is taken to be the same as the gas velocity. The concentration of the particulate phase is set to be uniform at the inlet. At the outlet the zero streamwise gradients are used for all variables. The wall boundary conditions are based on the model of Tu and Fletcher (1995).

Nominal Diameter(μm)	90	150	70
Material	Glass	Glass	Copper
Density(kg/m^3)	2500	2500	8800
Stokes Number (St)	3.7	7.4	7.1
Particle Reynolds number (Re_p)	2.7	9.0	4.0

Table 1. Properties of the dispersed phase

All the governing equations for both gas and particle phase are solved sequentially at each iteration. The solution process starts by solving the momentum equations of the gas phase followed by the pressure-correction through continuity. This is then followed by solution of turbulence equations for the gas phase, whereas the solution process for the particle phase starts by solving the momentum equations followed by the concentration and then by the gas-particle turbulence interaction and ends by solving the turbulence equation for the particulate phase. At each global iteration, each equation is iterated, typically 3 to 5 times, using a strongly implicit procedure (SIP). The above solution process is marched towards a steady state and is repeated until a converged solution is obtained.

RESULTS AND DISCUSSION

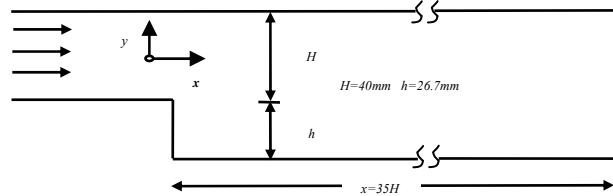


Fig.1 Backward facing step geometry

Figure 1 shows the schematic sketch of the test section used for the computations. As the span wise z -direction perpendicular to the paper is much larger than the y -direction

used in the experiments of Fessler and Eaton (1999) the flow is considered to be essentially two-dimensional. The backward facing step has an expansion ratio of 5:3. The Reynolds number over the step works out to be 18,400 calculated based on the centerline velocity and step height (h).

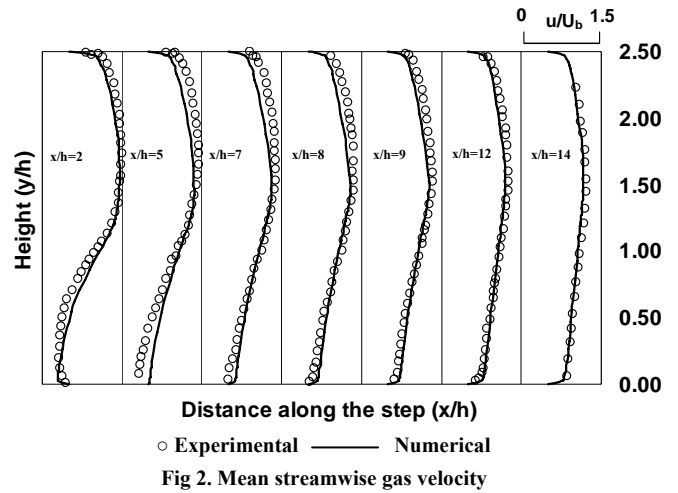


Fig 2. Mean streamwise gas velocity

Mean streamwise velocities: Figure 2 shows the mean streamwise gas velocities for various sections along the step, it can be seen that there is generally a good agreement with the experimental findings.

Figures 3-5 depict the mean streamwise velocity profiles of the three classes of particles that are considered in this study properties of which are tabulated in Table 1, an important parameter which characterizes the motion or the dispersion of the particulate phase in the presence of the carrier phase is the Stokes number ($\text{St} = \tau_p / \tau_f$); and it is defined as the ratio of the particle relaxation time that of the appropriate fluid time scale. It is also interesting to note that the 70 μm copper and the 150 μm glass particles share the same Stokes number.

Particle relaxation time is calculated using the formula $\tau_p = \frac{\rho_p d_p^2}{18\mu}$, where ρ_p and d_p are the density and diameter of the particles respectively. As the reattachment length is not constant in this study, it has not been considered as an appropriate length scale to calculate fluid time scale, rather a constant length scale of five step heights, which is in accordance to the reattachment length is used. The resulting time scale is given by $\tau_f = 5H/U_o$. Another important parameter used to describe the flow of particles is the particle Reynolds number (Re_p) which is given by $\frac{\rho_f |u_p - u_g| d_p}{\mu}$, where $|u_p - u_g|$ is the magnitude of the relative velocity.

From the particle mean velocity graphs it can be inferred, that the particle streamwise velocity at the first station $x/h=2$ is lower than the corresponding gas velocities, this is in lines with the fully developed channel flow reaching the step. This has been described in the experiments of Kulick et al (1994), wherein the particles at the channel centerline have lower streamwise velocities than that of the fluid as a result of cross-stream mixing.

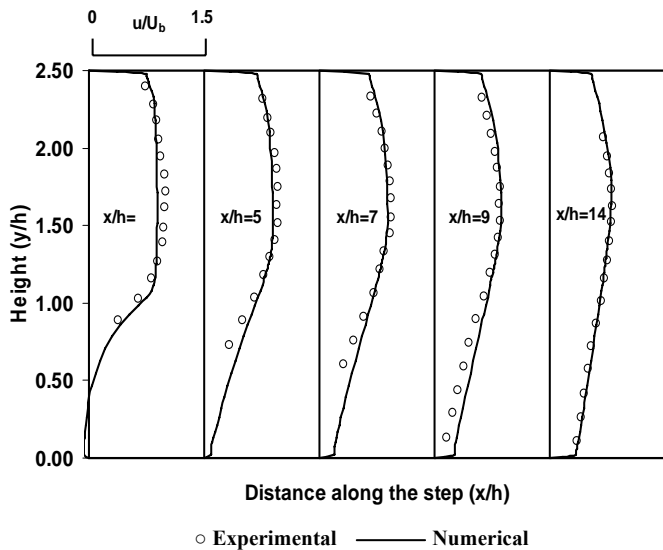


Fig.3 Streamwise mean velocity for 90µm glass particles

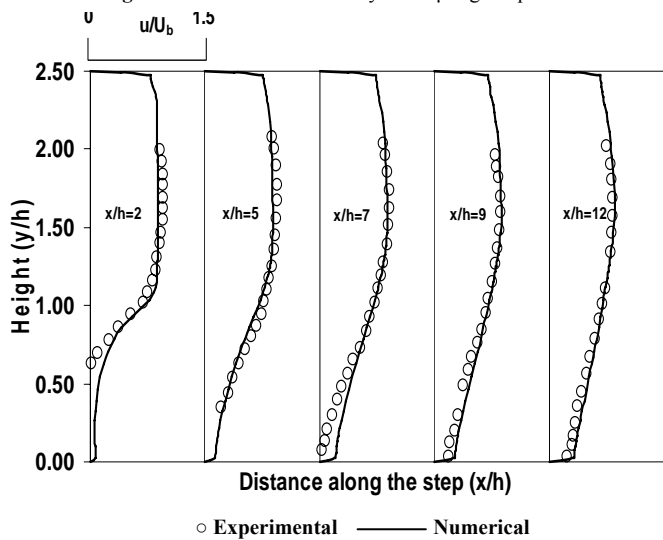


Fig.4 Streamwise mean velocity for 70µm copper particles

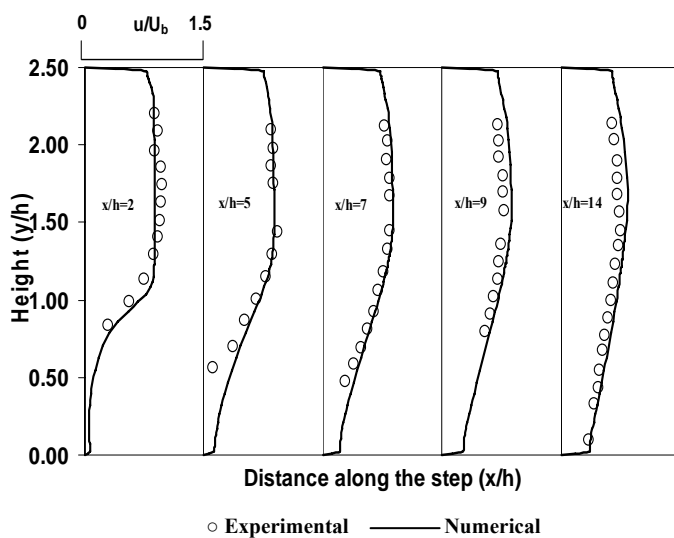


Fig.5 Streamwise mean velocity for 150µm glass particles

However the gas velocity lags behind the particle velocities aft of the sudden expansion as the particles inertia makes them slower to respond to the adverse pressure gradient than the fluid.

Mean streamwise fluctuations:

Figure 6 shows the streamwise fluctuating velocity profiles of the gas phase, it can be seen that the numerical results are found to obey the same trend as the experimental results, however there seems to be a general under-prediction of numerical results in comparison to the experimental values. This under prediction is more pronounced towards the lower wall for a height of up to $y/H \leq 2$.

Figures 7-9 shows the streamwise fluctuating particle velocities for the three different classes of particles considered, there is a general under-prediction for the streamwise fluctuating velocities for the 90µm glass particles but the results are found to be in accordance with the experimental findings. For the 70µm copper and 150µm glass particles which share the same Stokes number there has been a minor over-prediction until stations $y/H \leq 1$. All the experimental results used for comparison of particle fluctuating velocities correspond to maximum mass loadings of particles as reported in the experiments of Fessler & Eaton (1997).

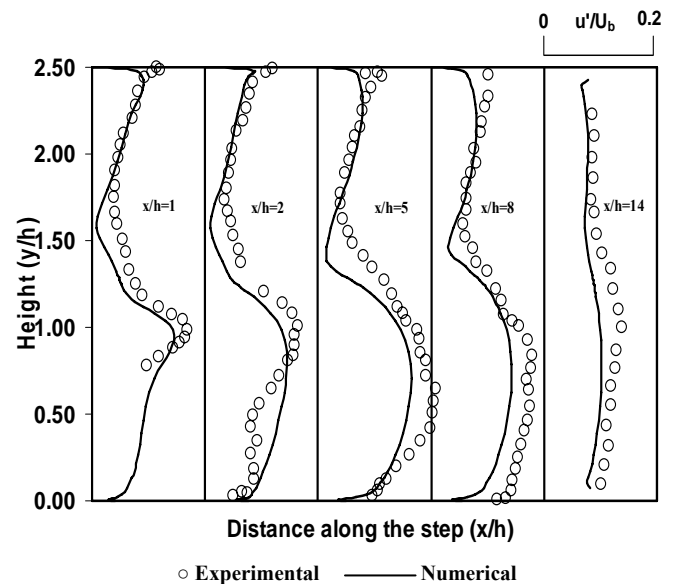


Fig.6 Fluctuating streamwise gas velocities

It can be also seen that for $y/H > 1.5$, the particle fluctuating velocities are considerably larger than those of the fluid. This again is in accordance with channel flow inlet conditions, where the particles have higher fluctuating velocities than those of the fluid owing to cross-stream mixing.

Mean particle concentration:

Particle number density (PND) results obtained from the numerical procedure are compared with the experimental findings of Fessler & Eaton (1999). The numerical results are obtained by normalizing by the maximum value and again by a non-dimensional number there by making it dimensionless.

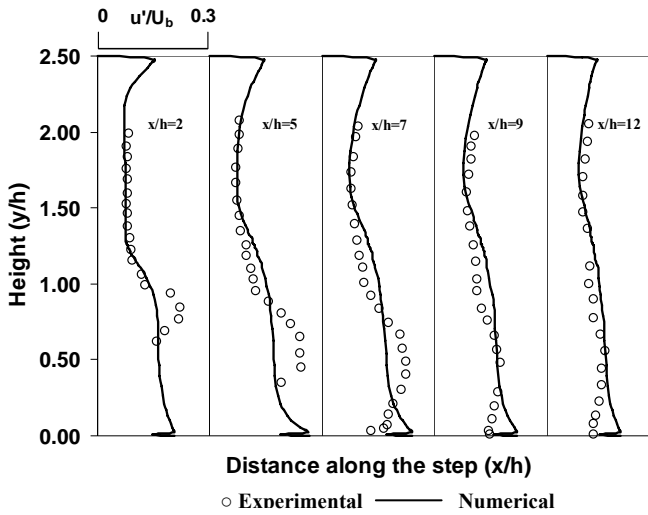


Fig.7 Fluctuating streamwise particle velocities for 90µm glass particles

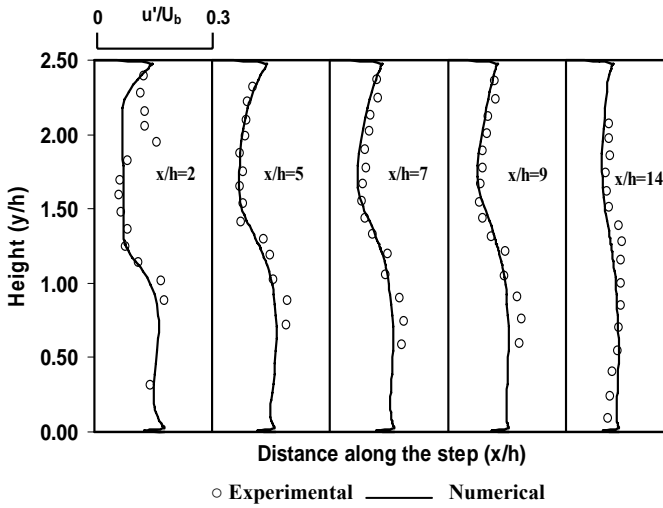


Fig.8 Fluctuating streamwise particle velocities for 70µm copper particles

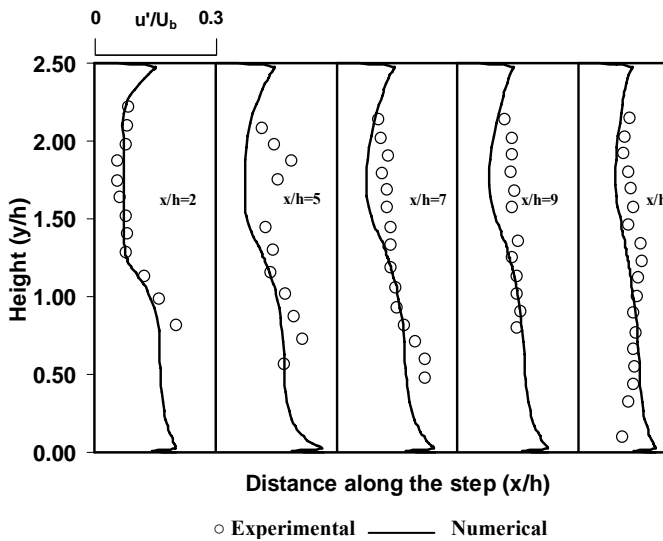


Fig. 9 Fluctuating streamwise particle velocities for 150µm glass particles

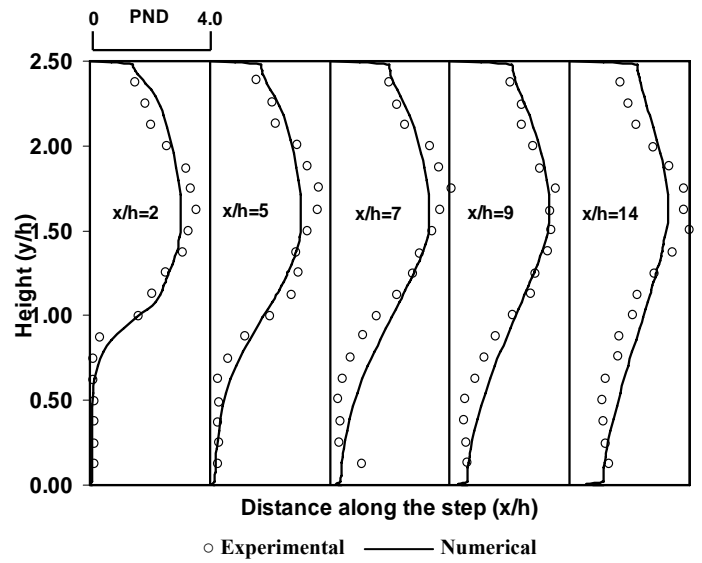


Fig.10 Particle number density for 90µm glass particle

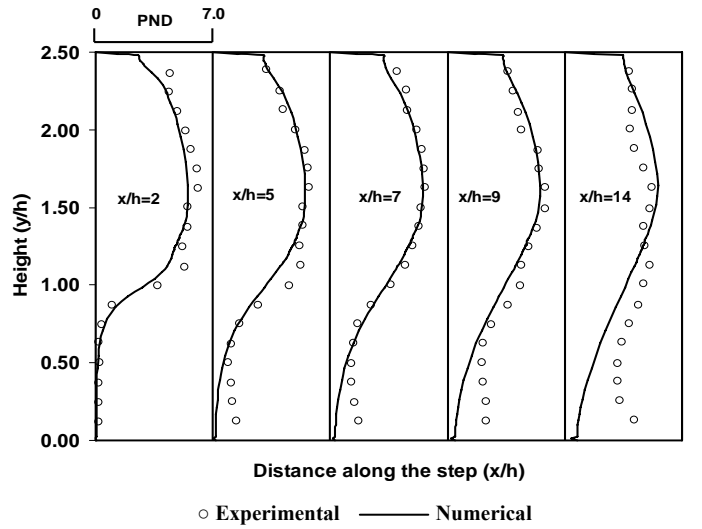


Fig.11 Particle number density for 70µm copper particles

It can be generally seen that from figures 10-12 that a fairly good agreement is seen for all the different classes of particles considered. However the numerical results predict fairly uniform number density for a region of $y/H > 1$, which is above the step and this phenomena is less pronounced with increasing distance along the step (x/h).

It can be observed from the plots that clearly there are very few particles found in the re-circulation zone for $y/h < 1$, this is not surprising because the Stokes number based on large-eddy time scale, are all larger than one (Fessler & Eaton, 1995), after this zone there is an increasing number of particles for $y/h < 1$ until at $x/h=15$, where the number density across the section becomes fairly uniform.

The key necessity of studying the distribution of the mean particle concentrations across the test section is attributed towards turbulence modification of the carrier phase; as the local particle concentration is known to have a strong effect on degree of turbulence modification.

Recirculation length characteristics:

This section shows the variation of reattachment point with the Stokes number and that of particle Reynolds number. In addition to the three classes of particles; extra two classes of glass particles of 25 μm and 50 μm diameter are considered. The main aim of investigating these additional particles is to study the preferential concentration behavior and also to increase the Stokes number range in the experiments of Fessler and Eaton (1999). However, their Stokes and particle Reynolds number have also been used to study the reattachment point in our current study.

Figure 12 shows the plot of the reattachment length for the particulate phase against Stokes number it can be seen that there is generally a decrease in the reattachment length with the increase in Stokes number. It can also be seen that there is a sharp dip in the reattachment length for 25 μm particle in close contrast to 50 μm particle.

Figure 13 shows the plot of the reattachment length plotted against Particle Reynolds number (Re_p). Reattachment length seems to decrease with the increase in the particle Reynolds number.

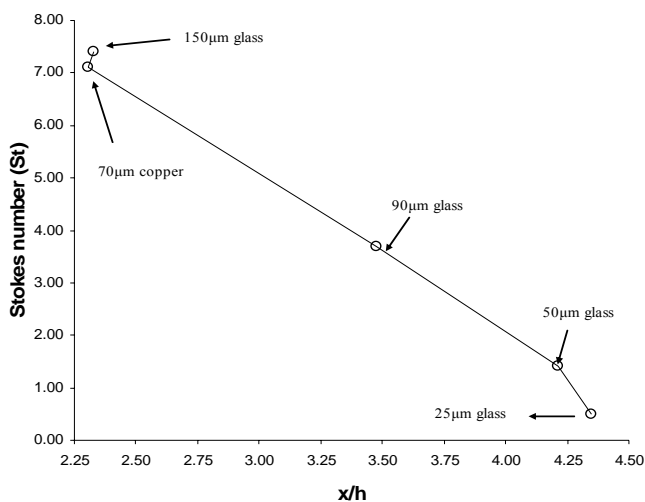


Fig.12 Re-attachment point Vs Stokes number

CONCLUSION

Numerical simulation for turbulent two-phase flow has been successfully investigated with the Eulerian two-fluid model. The simulated mean velocity results, fluctuating velocities along with the particle number density results for both carrier phase and the dispersed phase agree were compared against the experimental results of Fessler and Eaton (1995). The majority of the results agree well with the experimental data; however there have been some under prediction in certain sections of the step for fluctuating velocities and particle number density.

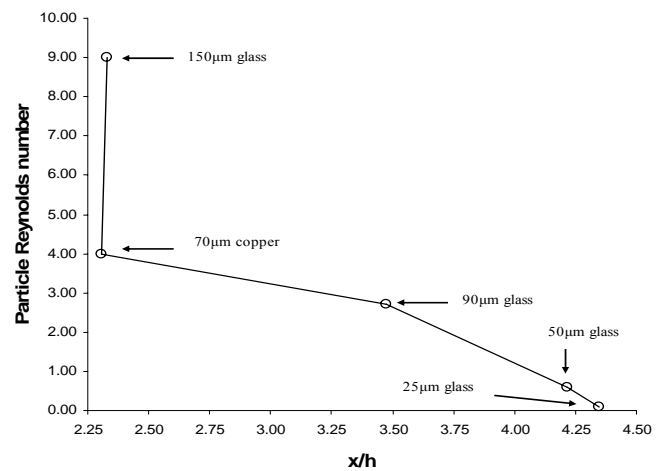


Fig.13 Re-attachment point Vs particle Reynolds number

The re-attachment point for the various class of particles have been plotted as a function of both Stokes number and particle Reynolds number, it is also seen that for particles with Stokes number less than one tend to disperse more within the carrier gas phase rather than for higher Stokes number.

ACKNOWLEDGEMENT

This work was partially supported by the DSTO and the first author was supported by IPRS research scholarship.

REFERENCES

- FESSLER, J. R. & EATON, J. K. (1995). Particle-turbulence interaction in a backward-facing step flow. *Mech. Engng Dept. Rep. MD-70*. Stanford University, Stanford, California
- FESSLER, J.R., & EATON, J. K. (1999). Turbulence modification by particles in a backward-facing step flow. *J.Fluid Mech.* 394, 97-117.
- KULICK, J. D., FESSLER, J. R. & EATON, J. K. (1994). Particle response and turbulence modification in fully developed channel flow. *J. Fluid Mech.* 277, 109-134.
- SCHUH, M.J., SCHULER, C.A., & HUMPHREY, J.A.C. (1989). Numerical Calculation of particle-laden gas Flows Past Tubes, *AIChE Journal*. 35(3), 466-480.
- TU, J.Y., & FLETCHER, C.A.J. (1995). Numerical Computation of Turbulent Gas-Solid Particle flow in a 90° Bend. *AIChE Journal*, 41 (10), 2187-2197.
- TU, J. Y. (1997). Computational of Turbulent Two-Phase Flow on Overlapped Grids. *Numer. Heat Transfer Part B Fundam.* 32, 175-195.
- YAKHOT, V., & ORSZAG, S.A. (1986) Renormalization group analysis of turbulence I. basic theory. *J. Sci. Comput.* 1, 3-51.